

Observability of the anapole moment and neutrino charge radius

M. J. Musolf

*Center for Theoretical Physics, Laboratory for Nuclear Science and Department of Physics,
Massachusetts Institute of Technology, Cambridge, Massachusetts 02139*

Barry R. Holstein

Department of Physics and Astronomy, University of Massachusetts, Amherst, Massachusetts 01003

(Received 25 September 1990)

The properties of the neutrino charge radius (NCR) and anapole moments (AM's) of elementary fermions, nucleons, and nuclei are discussed. The dependence of these off-shell electromagnetic couplings on the weak gauge parameter is explicitly demonstrated by a calculation performed in the R_ξ gauge. The gauge dependence of the AM's and NCR implies that they cannot be observed in isolation from other second-order, electroweak effects. It is shown, however, that the AM's of various hadronic systems having an $SU(2)_L$ quantum number $T_3^L=0$ can be considered "observables" in certain formal, though unphysical, limits. It is argued that, apart from these special limits, the AM is a physically meaningful entity only for heavy and/or nearly degenerate nuclei.

I. INTRODUCTION

Considerable interest has arisen recently in the so-called "anapole moment" (AM)—the leading parity-odd (P), time-reversal-even (T) electromagnetic coupling to a fermion or systems of fermions. First introduced by Zeldovich several decades ago,¹ the AM has received much less attention than its P - and T -odd counterpart, the electric dipole moment (EDM). The reasons are twofold. First, in contrast with the EDM, the AM cannot be probed by laboratory fields. Its only physical manifestation occurs in processes such as electron scattering which involve the exchange of virtual, neutral vector bosons (Z^0, γ). Second, since electromagnetism conserves parity in the absence of weak interactions, one expects an anapole term to enter low-energy, parity-nonconserving (PNC) amplitudes at $O(\alpha G_F)$ and parity-conserving amplitudes at $O(\alpha G_F^2)$. Until very recently, low-energy measurements of neutral-boson-exchange processes have not possessed the sensitivity needed to resolve effects of this order. However, improvements in the precision of atomic PNC experiments,² as well as the prospect of future high-precision PNC $\bar{e}N$ scattering experiments at intermediate-energy facilities such as the Continuous Electron Beam Accelerator Facility (CEBAF),³ suggest that observation of an AM might soon be experimentally feasible.

With this possibility in mind, we discuss below the AM's of elementary fermions (leptons and quarks), nucleons, and nuclei as well as a related electromagnetic coupling—the neutrino charge radius (NCR). Because some confusion persists with regard to the form and properties of these couplings, we first summarize their general features. In the remainder of the paper, we consider the observability of the AM and NCR. By a "physical observable," we will mean a quantity satisfying both of the following criteria.

(a) Within a given theoretical framework, it can be as-

signed a well-defined value.

(b) This value could, in principle, be determined experimentally.

With regard to these two criteria, we demonstrate that within the framework of the minimal $SU(2)_L \times U(1)_Y$ standard model, the NCR and AM's of elementary fermions are *not* well defined and possess no physical meaning when considered apart from physical processes involving exchange of virtual, neutral vector bosons. Moreover, contributions made by the AM and NCR to such processes are not generally distinguishable from other $O(\alpha G_F)$ contributions. In general, then, neither the NCR nor the AM of any system composed of elementary fermions can be considered physical observables under the above definition.

We find, however, that for the special case of fermionic systems having a total $SU(2)_L$ quantum number $T_3^L=0$, the AM *is* well defined. We show, moreover, that the AM's of various $T_3^L=0$, hadronic systems would in principle be experimentally measurable in several *formal*, though unphysical, limits: (a) for any $T_3^L=0$ hadronic system, when certain elementary-fermion masses $\rightarrow 0$; (b) for the isoscalar component of the nucleon, when the masses of pseudoscalar mesons and neutral vector mesons $\rightarrow 0$; and (c) for isoscalar nuclei, when the number of bound nucleons $\rightarrow \infty$. To the extent that these systems can be treated as having a *weak* isospin quantum number $T_3^L=0$, their AM's satisfy both criteria defining a physical observable in these formal limits.

Finally, we argue that the only physically realizable systems for which it makes sense to speak of an AM are very heavy nuclei and nuclei which possess pairs of nearly degenerate, opposite-parity states (we do not consider the AM's of molecules, which have been discussed elsewhere by Khriplovich⁴). Our conclusions are based on the following results.

(i) The AM of an elementary fermion depends in general on the choice of weak $SU(2)_L \times U(1)_Y$ gauge param-

ter ξ . Since the value of ξ is arbitrary, the AM is not a physical observable and must be considered in conjunction with all other ξ -dependent, $O(\alpha G_F)$ contributions to physical amplitudes. In contrast with the charge, magnetic moment, and EDM, the AM is *not* an intrinsic and well-defined property of an elementary particle. As has been known for some time, a similar conclusion also holds for the NCR.^{5–8} We demonstrate this result by giving explicit formulas for the lepton and quark AM's calculated in the R_ξ gauge. We also discuss the renormalization scheme dependence of the AM and NCR.

(ii) The ξ -dependent terms in the NCR and AM of an elementary fermion are proportional to T_3^L , the third component of the fermion's weak isospin. Thus, for fermionic systems which satisfy $T_3^L=0$, the ξ -dependent terms vanish and the AM is well defined.

(iii) The AM of an elementary fermion and the NCR contain ξ -independent terms which are logarithmically singular in the fermion masses m_f . Formally, various $m_f \rightarrow 0$ limits can be used to distinguish the AM of $T_3^L=0$ systems from other $O(\alpha G_F)$ terms in certain physical amplitudes. In a world defined by such limits, the AM would generate the dominant, ξ -independent contribution to neutral-current observables.

(iv) At the physical values of m_f , however, the logarithmic terms in the AM and NCR are in general numerically no more or less important than other second-order electroweak contributions to physical amplitudes. We find that only in the special case of parity-nonconserving (PNC) scattering involving a charged-lepton vector coupling do the ξ -independent fermion mass logarithms dominate the one-loop scattering amplitude.

(v) The nucleon AM contains additional, ξ -independent terms—generated by mesonic intermediate states—which are singular in the meson masses. In the $m_{\text{meson}} \rightarrow 0$ limit, these terms will dominate any scattering amplitude to which the nucleon AM contributes. To the extent that the presence of heavy quarks in the nucleon can be neglected, the isoscalar nucleon AM is both well defined and physically distinguishable in the $m_{\text{meson}} \rightarrow 0$ limit.

(vi) At the physical values of m_{meson} , however, contributions made by mesonic terms of (v) to scattering ampli-

tudes are numerically of the same scale as other second-order electroweak corrections.

(vii) In general, the above conclusions also hold for the *nuclear* AM. Because it receives contributions from the ξ -dependent quark AM's, the nuclear AM is well defined only for $T_3^L=0$ nuclei. The $m_f \rightarrow 0$ and $m_{\text{meson}} \rightarrow 0$ limits would render the AM of such nuclei physical observables. In addition, recent calculations by Flambaum, Khriplovich, and Sushkov⁹ and by Haxton, Henley, and Musolf¹⁰ indicate that nuclear AM contains a ξ -independent *many-body* term whose magnitude grows as the two-thirds power of the mass number A . Thus, the $A \rightarrow \infty$ limit constitutes a third formal limit in which the AM of $T_3^L=0$ nuclei would be physical observables.

(viii) For finite values of A , the many-body component of the AM of special heavy nuclei or nuclei possessing pairs of nearly degenerate, opposite-parity states may generate the largest contribution to PNC scattering amplitudes sensitive to the nuclear spin. These special nuclei constitute the one *physically realizable* case for which it makes sense to speak of an AM in distinction from other second-order, electroweak effects.

In the remainder of the paper, we expand upon these points. In Sec. II, we carefully define the AM and NCR and discuss their general properties. In Sec. III, we discuss our calculation of the elementary fermion AM and NCR. In the following two sections, we consider the implications of this calculation for PNC scattering amplitudes and for the AM's of $T_3^L=0$ hadronic systems, respectively. Section VI contains a more detailed treatment of the nucleon AM. In Sec. VII, we discuss briefly the features of the AM's of nuclei. The final section summarizes our main conclusions.

II. GENERAL FEATURES

Lorentz covariance and electromagnetic gauge invariance imply that the AM cannot be probed in isolation from neutral-current interactions. These symmetries require matrix elements of the em current for a spin- $\frac{1}{2}$ fermion to have the general form

$$e \langle p' | J_\mu^{\text{em}}(0) | p \rangle = e \bar{u}(p') \left[F_1(q^2) \gamma_\mu - i \frac{F_2(q^2)}{2M} \sigma_{\mu\nu} q^\nu + \frac{F_A(q^2)}{M^2} (q^2 \gamma_\mu - \not{q} q_\mu) \gamma_5 - i \frac{F_E(q^2)}{2M} \sigma_{\mu\nu} q^\nu \gamma_5 \right] u(p), \quad (1)$$

where $q = p - p'$ and M is the fermion mass (for massless neutrinos, we take $M = m_l$, where m_l is the mass of the corresponding charged lepton). The terms containing $F_1(q^2)$ and $F_2(q^2)$ are the usual charge and anomalous magnetic-moment terms, respectively. In the absence of parity- and/or time-reversal-violating interactions, these are the only terms allowed by the parity-conserving electromagnetic interaction. Weak radiative corrections to the tree-level fermion-photon vertex allow for the possibility of two additional terms in the matrix element (1). The term containing $F_E(q^2)$ is the electric dipole term, and its coupling to a photon is both parity and time-

reversal violating. The final term, containing the form factor $F_A(q^2)$, is the anapole term. Its coupling to a photon violates parity but preserves time-reversal invariance. Since the experiments mentioned in Sec. I all involve relatively low- q^2 processes, we focus on the static, dimensionless AM, $F_A(0)$. By contracting (1) with a photon of polarization $\epsilon^\mu(q)$ and taking the Fourier transform, it is straightforward to derive the coordinate space form for the low- q^2 anapole interaction:

$$\mathcal{L}^{\text{anapole}} = -e \frac{F_A}{M^2} \bar{\psi} \gamma_\mu \gamma_5 \psi \partial_\lambda F^{\mu\lambda}, \quad (2)$$

where ψ and $F^{\mu\lambda}$ are the fermion field and em field tensor, respectively, and F_A is the dimensionless anapole moment.

Two features of the anapole coupling follow directly from Eqs. (1) and (2). First, since $q^2=0$ and $\epsilon\cdot q=0$ for real photons, Eq. (1) implies that the anapole interaction is nonvanishing only when the photon is virtual. Second, in low- q^2 processes involving virtual γ exchange, this interaction generates a contact interaction between the fermion and the source of the virtual particles. This feature follows most directly from Eq. (2). Applying the photon equations of motion, $\partial_\lambda F^{\mu\lambda}=ej^\mu$, where j^μ is the source of virtual photons, one obtains a contact interaction between an axial-vector fermion current and the source current. This current-current interaction has the same form as that generated by low- q^2 Z^0 exchange, and like the latter, it is nonvanishing only when the fermion and

the source coincide spatially. Furthermore, any source j^μ of virtual photons will also emit virtual Z^0 's, so that the low- q^2 anapole interaction always occurs in tandem with low- q^2 neutral-current processes involving an axial-vector coupling to the fermion. From this standpoint, the AM manifests itself physically as an $O(\alpha)$ correction to tree-level neutral-current interactions.

As pointed out in Ref. 10, these two properties also apply to the AM of a system of bound fermions having spin $J \geq \frac{1}{2}$. In the context of the multipole expansion, which provides a natural framework for analyzing electromagnetic interactions of such systems, the anapole coupling is identified with the leading P -odd/ T -even, *elastic* transverse electric multipole moment: $T_{L=1}^E$.¹¹ As expressed by Siegert's theorem,¹²⁻¹⁴ current conservation requires this multipole to have the form

$$T_{L=1}^E \Big|_{Q^2 \rightarrow 0}^{\text{elastic}} \rightarrow -i \frac{Q^2}{9\sqrt{6}\pi} \left\langle \text{g.s.} \left| \int d^3r r^2 \{ \mathbf{J}(\mathbf{r})^{\text{em}} + \sqrt{2\pi} [Y_2(\Omega_r) \otimes \mathbf{J}(\mathbf{r})^{\text{em}}]_1 \} \right| \text{g.s.} \right\rangle, \quad (3)$$

where \mathbf{J}^{em} is a current operator, $\langle \text{g.s.} | \hat{\mathcal{O}} | \text{g.s.} \rangle$ denotes a reduced ground-state matrix element, $Q^2 \equiv |\mathbf{q}|^2$, and \otimes is a tensor product. For elastic processes, one has $q_0=0$ (neglecting recoil) so that $q^2 = -Q^2$. Thus, (3) vanishes for *real* photons but, when combined with the $1/q^2 = -1/Q^2$ photon propagator, generates a contact interaction between a source of *virtual* photons and the system of fermions.

For the left-handed Dirac neutrinos of the standard model, the NCR and neutrino AM are identical (up to factors associated with conventions adopted in defining these couplings). The NCR is conventionally defined as

$$\langle r^2 \rangle_{\text{em}}^{(\nu)} = 6 \frac{dF_1^{(\nu)}}{dq^2} \Big|_{q^2=0}, \quad (4)$$

where $F_1^{(\nu)}(q^2)$ is the neutrino charge form factor. Expanding $F_1^{(\nu)}(q^2)$ in powers of q^2 , noting that $F_1^{(\nu)}(0)=0$, and using the definition (4) leads to the following form for the neutrino matrix element of the em current:

$$\langle \nu(p') | J_\mu^{\text{em}} | \nu(p) \rangle = \frac{1}{6} e \langle r^2 \rangle_{\text{em}}^{(\nu)} \bar{u}_\nu(p') q^2 \gamma_\mu u_\nu(p), \quad (5)$$

where higher-order terms in q^2 and a possible magnetic-moment term have been neglected. Now observe that for massless, on-shell fermions, one has

$$\bar{u} \not{q} \gamma_5 u = 0 \quad (6)$$

so that the second-term in the anapole coupling in Eq. (1) is zero. Moreover, for left-handed fermions,

$$\bar{u} \not{L} \gamma_\mu \gamma_5 u^L = -\bar{u} \not{L} \gamma_\mu u^L. \quad (7)$$

Thus, from (4)–(7) and (2) it immediately follows that for the massless, left-handed neutrinos of the standard model, the NCR is just $-\frac{1}{6}$ times the anapole coupling F_A/M^2 . (We note that this identity does *not* apply to Majorana neutrinos ν_M . It has been shown previously

that the anapole form factor is the only electromagnetic form factor which a ν_M may possess.¹⁵)

This result suggests a natural interpretation of the anapole coupling F_A/M^2 as an axial electromagnetic charge radius squared $\langle r^2 \rangle_5^{\text{em}}$. As it appears in Eq. (1), the scale of $\langle r^2 \rangle_5^{\text{em}}$ is set ostensibly by M^{-2} , where M is the particle mass. For leptons and quarks, however, we find that F_A is proportional to $(M/M_{Z,W})^2$, so that the heavy-vector-boson masses actually govern the scale of these AM's. For nucleons, we find that F_A/m_N^2 contains powers of m_N/m_{meson} , so that meson masses, as well as m_N , play a role in setting the scale of the nucleon $\langle r^2 \rangle_5^{\text{em}}$. In contrast with the situation for individual fermions, the anapole coupling of an *extended* system of fermions—such as a nucleus—can depend more strongly on the spatial extent of the system than on the total mass or the masses of the fermion constituents. This result follows from the form of the multipole operator in Eq. (3), which gives the anapole coupling as an r^2 -weighted moment of the three-current. Consequently, it would be reasonable to expect the nuclear AM to grow as $\langle r^2 \rangle_{\text{nuclear}} \sim r_0^2 A^{2/3}$, where $r_0 \approx 1.2$ F and A is the number of bound nucleons. In fact, this result was first demonstrated by the authors of Ref. 9 for nuclei in which the weak interaction mixes opposite-parity states into the ground state. The authors of Ref. 10 later showed that the meson-exchange current contribution to the nuclear AM displays the same $A^{2/3}$ behavior.

III. ELEMENTARY-FERMION ANAPOLE MOMENT

We have estimated F_A for elementary fermions of the standard model by calculating the one-loop amplitudes associated with Fig. 1. Working within the framework of the minimal $SU(2)_L \times U(1)_Y$ standard model having a single Higgs doublet, we performed the calculation in the

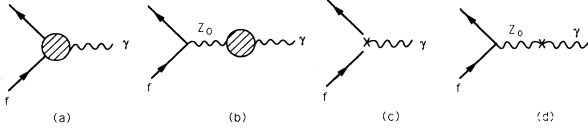


FIG. 1. Contributions to the AM of an elementary fermion f and the charge radius of the neutrino. The shaded circles in (a) and (b) denote one-loop contributions to axial-vector vertex corrections and the Z - γ mixing tensor, respectively. (c) and (d) represent the corresponding one-loop counterterms.

general R_ξ gauge¹⁶ in order to demonstrate the gauge dependence of F_A . Because the one-particle-irreducible two- and three-point amplitudes contained in Figs. 1(a) and 1(b) are UV divergent, they contribute to the renor-

malization of the classical $SU(2)_L \times U(1)_Y$ Lagrangian. We carried out the renormalization using dimensional regularization and an on-shell renormalization (OSR) scheme.¹⁷ The OSR counterterms [Figs. 1(c) and 1(d)] render the amplitudes finite and regulator independent and preserve the symmetry of the classical theory.¹⁸ We note that the sum of the axial-vector corrections [Figs. 1(a) and 1(c)] and Z - γ mixing term [Figs. 1(b) and 1(d)] is needed in order to obtain the gauge-invariant form of Eq. (1). In particular, the longitudinal component of the renormalized Z - γ mixing tensor, $B_{Z\gamma}(q^2)q^\mu q^\nu / q^2$, cancels a gauge-noninvariant term in the renormalized, axial-vector fermion-photon vertex. A more detailed discussion of our calculation will appear elsewhere,¹⁹ and we simply quote here our results for $F_A = \sum_{i=1}^4 F_A^{(i)}$:

$$\begin{aligned}
 F_A^{(1)} &= -\frac{\alpha}{(4\pi)} \left[\frac{m_f}{M_Z} \right]^2 \left[\frac{1}{4 \cos\theta_W \sin\theta_W} \right]^2 g_A^f \left[9 - \frac{115}{9} \cos^2\theta_W - \frac{5}{9} \sin^2\theta_W - (\xi-1)(1+2 \cos^2\theta_W) \right. \\
 &\quad \left. - \left[\frac{16}{3} - \frac{46}{3} \cos^2\theta_W - \frac{2}{3} \sin^2\theta_W - 4(\xi-1) + \frac{6}{\xi-1} (1-2 \cos^2\theta_W) \right] \ln\xi \right], \\
 F_A^{(2)} &= -g_A^f \left[\frac{m_f}{M_Z} \right]^2 \left[\frac{1}{4 \cos\theta_W \sin\theta_W} \right] \left\{ \frac{\alpha}{(4\pi)} \left[\frac{\cos\theta_W}{\sin\theta_W} \right] \left[\frac{3}{2} + \frac{1}{4} (\xi-1) - \left[\frac{3}{2} \frac{1}{\xi-1} + \frac{1}{2} (\xi-1) + 2 \right] \ln\xi \right] \right. \\
 &\quad \left. - \frac{1}{M_Z^2} \bar{A}_{Z\gamma}(\xi; M_Z^2) \right\}, \\
 F_A^{(3)} &= \frac{\alpha}{(4\pi)} \left[\frac{m_f}{M_Z} \right]^2 \left[\frac{1}{4 \cos\theta_W \sin\theta_W} \right]^2 \frac{4}{3} \left[Q_f g_V^f g_A^f \left[\frac{1}{6} - \ln \frac{m_f^2}{M_Z^2} \right] - 2 \sum_{f'} Q_{f'} |U_{ff'}|^2 \left[\frac{1}{6} - \ln \frac{m_{f'}^2}{M_W^2} \right] \right], \\
 F_A^{(4)} &= -\frac{\alpha}{(4\pi)} \left[\frac{m_f}{M_Z} \right]^2 \left[\frac{1}{4 \cos\theta_W \sin\theta_W} \right]^2 \frac{4}{3} g_A^f \sum_{f'} Q_{f'} g_V^{f'} N_c^{f'} \ln \frac{m_{f'}^2}{M_W^2},
 \end{aligned} \tag{8}$$

where the Weinberg angle is defined²⁰ by $\sin^2\theta_W \equiv 1 - M_W^2/M_Z^2$; Q_f , T_3^f , and m_f are the charge, $SU(2)_L$ quantum number, and mass, respectively, of fermion f (recall that $m_f \rightarrow m_l$ when f is a massless neutrino); $g_V^f = 2T_3^f - 4Q_f \sin^2\theta_W$ and $g_A^f = -2T_3^f$ are the vector and axial-vector neutral-current couplings, respectively; $U_{ff'}$ are entries in the Kobayashi-Maskawa (KM) matrix; N_c^f is the number of ‘‘colors’’ of fermion f ; and $\bar{A}_{Z\gamma}(M_Z^2)$ is a regulator-independent part of the transverse Z - γ mixing tensor, evaluated at $q^2 = M_Z^2$. The masses $m_{f'}$ in $F_A^{(3)}$ correspond to the weak isospin partner(s) of fermion f (e.g., $m_{f'} = m_e$ when $f = \nu_e$). The sum in $F_A^{(4)}$ is over all species of fermions. Finally, when considering the lepton AM or NCR, we set $U_{ff'} \rightarrow \delta_{ff'}$.

We have separated the AM and NCR into the four contributions $F_A^{(i)}$ in order to highlight different features of these couplings. The most significant of these is the dependence of the AM on the weak gauge parameter ξ shown explicitly in $F_A^{(1)}$ and $F_A^{(2)}$. The terms in $F_A^{(1)}$ result from a ξ -dependent subset of the one-loop graphs appearing in Figs. 1(a) and 1(b). The terms in $F_A^{(2)}$ correspond to

UV finite parts of the counterterms [Figs. 1(c) and 1(d)] which remain in the normalized $ff\gamma$ three-point function after the divergences of Figs. 1(a) and 1(b) are canceled by the regulator-dependent parts of the counterterms. The gauge dependence enters these graphs through the vector boson, unphysical scalar (Higgs) boson, and ghost particle propagators. The first of these, for example, has the form, in the R_ξ gauge,

$$\Delta_{\mu\nu}(q^2) = \frac{-i}{q^2 - M_V^2 + i\epsilon} \left[\eta_{\mu\nu} + (\xi-1) \frac{q_\mu q_\nu}{q^2 - \xi M_V^2} \right],$$

where M_V is the Z^0 or W mass. The unphysical particle propagators have analogous forms.

The gauge dependence of the electron AM was first noted by Czyz, Kolodziej, and Zralek²¹ who calculated F_A^{electron} using three specific choices of ξ . Previously, Dombey and Kennedy²² had calculated the electron AM in the Feynman-'t Hooft gauge ($\xi=1$) but did not note the gauge dependence. Our calculation generalizes that of Ref. 21, exhibiting explicitly the gauge dependence of

F_A for any elementary fermion of the standard model in the R_ξ gauge framework. Because the charge radius and AM of massless, left-handed neutrinos are proportional, our results also demonstrate the ξ dependence of the NCR—a fact which has been noted previously by several authors.^{6–8}

The primary implication of the gauge dependence of $F_A^{(1)}$ and $F_A^{(2)}$ is that the NCR and elementary-fermion AM's are not well defined. They can take on any value, depending on the choice of ξ . In the unitary ($\xi \rightarrow \infty$) gauge, for example, they are infinite. Only when embedded in a physical S -matrix element, where other gauge-dependent amplitudes cancel the ξ dependence of $F_A^{(1)}$ and $F_A^{(2)}$ (Fig. 2), do the AM and NCR have any physical significance. From this standpoint, then, the AM and NCR are more appropriately conceptualized as simply two types of electroweak radiative corrections to tree-level, Z^0 -exchange processes rather than as fundamental, well-defined properties of elementary particles. [The authors of Ref. 8 have defined an “effective” NCR by considering the full set of one-loop radiative corrections in neutrino scattering. However, although it is a gauge-independent quantity, this effective NCR neither represents a purely electromagnetic coupling nor, when embedded in a scattering amplitude, does it generate the full set of $O(\alpha G_F)$ contributions.]

In addition to depending on the choice of weak gauge, the NCR and AM are also renormalization-scheme dependent. This result is illustrated by $F_A^{(2)}$, which contains the finite counterterm contributions corresponding to Figs. 1(c) and 1(d). The precise form of this term depends on the renormalization scheme in use. In the OSR scheme employed in the present calculation, for example, all subtractions are carried out with particles on their mass shells, so that no extra finite renormalization factors are required on external particle legs. In this respect, our calculation differs from the electron AM calculation of Dombey and Kennedy,²² in which a renormalization scheme requiring finite renormalization factors on exter-

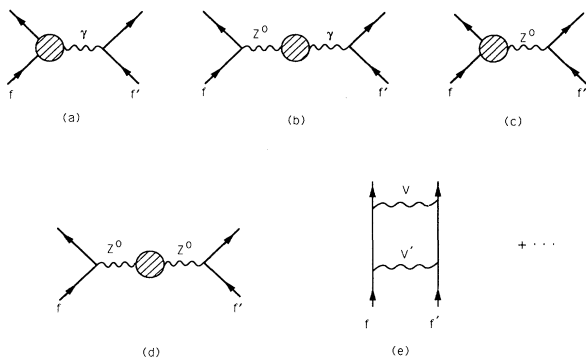


FIG. 2. Second-order electroweak corrections to tree-level, scattering amplitudes involving elementary fermions (f, f') of the standard model. (a) and (b) contain contributions from the AM of fermion f . The remaining diagrams are illustrative and do not represent the full set of corrections. Here $V, V' = Z^0, \gamma, W^\pm$, and shaded circles represent renormalized two- and three-point amplitudes.

nal legs was used. This difference in renormalization scheme choice may explain the difference between our $F_A(\xi=1)^{\text{electron}}$ and the result of Ref. 22.

We also note that not all terms appearing $F_A^{(2)}$ contribute to physical processes. In particular, the term containing $\bar{A}_{Z\gamma}(\xi; q^2 = M_Z^2)$ will not contribute to fermion-fermion scattering amplitudes,¹⁹ since $-\bar{A}_{Z\gamma}(\xi; q^2 = M_Z^2)$ appears in the counterterm for renormalization of the Z^0 -fermion vertex. When the two graphs in Fig. 3 are added, $\bar{A}_{Z\gamma}(\xi; q^2 = M_Z^2)$ cancels from the full amplitude. The appearance of $\bar{A}_{Z\gamma}(\xi; q^2 = M_Z^2)$ in F_A is simply an artifact of the particular renormalization conditions imposed on the Z - γ mixing tensor. Its cancellation from scattering amplitudes illustrates how particularities of a renormalization scheme which appear in F_A may be misleading when one seeks to analyze the physical consequences of the AM and NCR. Such renormalization scheme ambiguities constitute a second reason why the elementary fermion AM and NCR should be treated simply as part of the electroweak radiative corrections rather than as physical observables.

The terms contained in $F_A^{(3,4)}$ are ξ independent and logarithmically singular in fermion masses. Because these logarithms involve ratios of significantly different mass scales, $F_A^{(3)}$ and $F_A^{(4)}$ generate relatively large contributions to scattering amplitudes in which the AM and NCR appear. Since the interpretation of the m_f appearing in $F_A^{(3)}$ and $F_A^{(4)}$ differs in some respects, we discuss each case separately. The fermion mass logarithms in $F_A^{(3)}$ arise from the vertex correction graphs of Fig. 4(a). To leading order in q^2/M_Z^2 , the entire amplitude associated with these graphs is ξ independent. We denote the masses appearing in $F_A^{(3)}$ as “external” masses since they correspond to the external, asymptotic fermion f (the first term in $F_A^{(3)}$) or its weak-isospin partner(s) f' (the second term in $F_A^{(3)}$). In the NCR, for example, $Q_\nu = 0$ so that only the second term in $F_A^{(3)}$ contributes. In this case, one has $m_f^{\text{external}} = m_e$. For the electron AM, only the first term contributes, so that m_f^{external} is also identified with m_e . The external masses appearing in the AM of a quark q include both the m_q^{external} of q itself (the first term in $F_A^{(3)}$) as well as the m_q^{external} of all quarks carrying opposite weak isospin (the second term). We note that for a light-quark (u, d, s) AM, the heavy-quark contributions to $F_A^{(3)}$ are suppressed by the KM factors, $|U_{ff'}|^2$.

The fermion mass logarithms appearing in $F_A^{(4)}$ are gen-

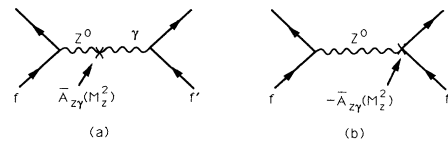


FIG. 3. Cancellation of finite counterterms from the full scattering amplitude.

erated by closed fermion loops illustrated in Fig. 4(b). We refer to these closed-loop masses as ‘‘internal’’ masses, m_f^{internal} . The m_f^{internal} logarithms must be ξ independent since no other diagrams exist in one-loop amplitudes which involve a sum over all charged fermions and contain the appropriate product of quantum numbers ($Q_f g_f^f$), as would be required to cancel a ξ dependence in $F_A^{(4)}$.

Distinguishing between m_f^{external} and m_f^{internal} is useful not only for purely conceptual reasons, but also for purposes of estimating the contributions of $F_A^{(3)}$ and $F_A^{(4)}$ to physical processes. In carrying out such estimates, one must make an appropriate choice for the m_f . Since lepton masses are known, this choice is unambiguous; both the internal and external lepton masses are identified with the physical lepton masses. For quarks, however, the choice is more problematic, since quarks cannot be observed in isolation. In a valence-quark picture of hadrons, for example, low- q^2 , virtual vector bosons exchanged between a hadron and a charged-lepton probe couple to dressed, valence quarks rather than to the ‘‘current’’ quarks of \mathcal{L}_{QCD} . Consequently, the external masses appearing in the quark AM’s should characterize bound, valence quarks. For a hadron of size ~ 1 F, for instance, the uncertainty principle constrains valence-quark momenta to be $\gtrsim 330$ MeV/ c . In this case, use of the constituent quark masses for m_q^{external} effectively suppresses the contribution of momenta below 330 MeV/ c to the loop integrals which generate the $F_A^{(3)}$.

The quarks appearing in the closed loops of Fig. 4(b) are not bound, so the uncertainty principle does not constrain their momenta. For this reason, it does not make sense to treat m_q^{internal} as a low-momentum cutoff or to identify the internal quark masses with the constituent masses. At first glance, it might seem more reasonable to use the current quark values for the m_q^{internal} . The strong interaction, however, implies otherwise. Since $F_A^{(4)}$ is obtained by evaluating fermion loop integrals at $q^2=0$, gluonic corrections to the simple fermion loops of Fig. 5 could be significant.²³ Whatever values one uses for the m_q^{internal} in $F_A^{(4)}$ should effectively account for these corrections.

The practical question arises as to how to estimate gluonic corrections, such as those illustrated in Fig. 5. Because these gluonic processes cannot be reliably calculated in perturbation theory at momentum scales where the strong coupling $\alpha_s(\mu)$ is large, other approaches for

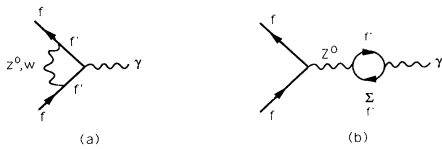


FIG. 4. Graphs generating ξ -independent, fermion mass logarithms appearing in $F_A^{(3,4)}$. Vertex corrections in (a) depend on external masses, whereas fermion loops in (b) generate internal mass dependence. The sum $\sum_{f'}$ involves small elementary fermions of the standard model.

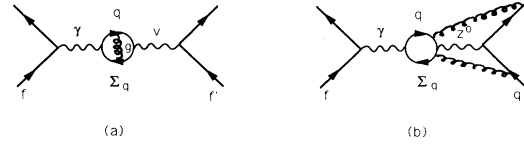


FIG. 5. Gluon corrections to closed fermion loops. Here, V denotes either a γ or Z^0 . The sum \sum_q is over all species of quarks. Corrections of type (a) occur in all fermion-fermion scattering amplitudes. Corrections of type (b) occur only for scattering in which at least one fermion is a quark.

estimating their magnitude must be taken. Corrections of the type in Fig. 5(a), where the vector boson V is a photon, can be estimated using a dispersive analysis of $R(e^+e^- \rightarrow \text{hadrons})$. As discussed in more detail below, the derivative of the unrenormalized, one-loop photon propagator, $A'_{\gamma\gamma}(q^2=0)$, also contains internal mass logarithms, and the values of m_q^{internal} appearing in the one-loop result for $A'_{\gamma\gamma}(0)$ can then be fit to reproduce the value of $R(e^+e^- \rightarrow \text{hadrons})$ via the dispersion relation. Such a procedure has been carried out by Hollik, yielding effective masses for the light quarks:²³

$$m_u = m_d = 41 \text{ MeV}, \quad m_s = 150 \text{ MeV}.$$

These values can be used to *define* what one means by m_q^{internal} and substituted into the sum in $F_A^{(4)}$. An alternate approach for estimating the corrections illustrated in Fig. 5(a) in the case where $V=Z^0$ has been developed by Marciano and Sirlin.²⁴ Their calculation, which accounts for the different isospin structure of $A_{Z\gamma}$, leads to somewhat different values for the internal quark masses: $m_u = m_d \approx 75$ MeV and $m_s \approx 250$ MeV. In neither approach, however, have gluonic effects illustrated by Fig. 5(b) been included. Note that while the corrections of Fig. 5(a) contribute to the AM’s of both leptons and quarks as well as to the NCR, those of Fig. 5(b) are relevant only to the quark AM’s.

IV. THE AM AND NCR IN SCATTERING AMPLITUDES

Rigorously speaking, the ξ -independent logarithms in $F_A^{(3,4)}$ cannot be unambiguously identified with the AM or NCR. Indeed, by a suitable choice of ξ , one could eliminate such terms altogether from $F_A^{\text{tot}} = \sum_{i=1}^4 F_A^{(i)}$ and reassign them to other ξ -dependent graphs in the complete one-loop amplitude.²⁵ Their physical significance lies in their contribution to the full amplitude and *not* in their assignment to a particular subset of one-loop diagrams. Nevertheless, it is instructive to ask about the numerical importance of these contributions to various physical processes. In a previous work, we discussed the full set of one-loop radiative corrections to PNC ff' scattering.¹⁸ In that analysis, we characterized the radiative corrections in terms of ratios $R \equiv A_{\text{PNC}}^{\text{rad}} / A_{\text{PNC}}^{\text{tree}}$, where $A_{\text{PNC}}^{\text{tree}}$ and $A_{\text{PNC}}^{\text{rad}}$ are the Born-level and one-loop PNC scattering amplitudes, respectively. Our results indicate that $F_A^{(3)}$ is numerically significant only in the special cases of $A(v_e) \times V(\mu)$ and $A(v_e) \times V(u)$ scattering,

where V and A denote vector and axial-vector couplings, respectively, to the particle indicated.

A significantly larger contribution is made to R by $F_A^{(4)}$ in $V(l) \times A(f)$ scattering, where l is a charged lepton and f is any elementary fermion. In such processes, the importance of the gauge-independent fermion mass logarithms is significantly enhanced relative to other one-loop contributions. The reasons for this enhancement are twofold. First, when the internal and external fermion masses are identified as described above, the m_f logarithms can be large—on the order of 10–20. Second, the one-loop photon-exchange diagrams involve a coupling to the lepton charge, $Q_l = -1$, whereas most of the remaining one-loop corrections contain the neutral-vector-current coupling $g_V^l = -1 + 4 \sin^2 \theta_w$, which is small. This difference in couplings to the lepton vector current enhances the relative importance of the photon-exchange contribution by roughly $Q_l/g_V^l \approx 13$. In the case of $V(\mu) \times A(\nu_e)$ scattering, the contributions from $F_A^{(3)}$ and $F_A^{(4)}$ cancel to a large extent.

In a few cases, other types of radiative corrections may enter at the same scale as the large fermion mass logarithms. Of particular interest are the Z - γ “box” graphs, which contain large logarithms in the fermion momenta. This contribution is especially significant in $V(e) \times A(u, d)$ scattering. In addition, other internal-mass logarithms can contribute to one-loop amplitudes, depending on how one chooses the set of independent parameters in the standard model. Specifically, if one takes (α, M_Z, M_W) as the independent parameters in the gauge-boson sector, then renormalized, one-loop weak amplitudes will contain a second sum over internal mass logarithms. This sum arises from the derivative of the unrenormalized, one-loop inverse photon propagator, $A'_{\gamma\gamma}(q^2=0)$:

$$\left. \frac{\partial A_{\gamma\gamma}(q^2)}{\partial q^2} \right|_{q^2=0} = \frac{\alpha}{(4\pi)} \frac{4}{3} \sum_f N_c^f Q_f^2 \ln \frac{m_f^2}{M_W^2} + \dots \quad (9)$$

Because the renormalized photon propagator is defined to have a pole with unit residue at $q^2=0$, $A'_{\gamma\gamma}(0)$ does not contribute to renormalized, parity-conserving electromagnetic amplitudes. It does appear, however, in weak-neutral-current amplitudes as part of the OSR counterterm needed to renormalize the one-loop Z^0 -fermion vertex.¹⁹ One may eliminate $A'_{\gamma\gamma}(0)$ fermion-fermion weak-neutral-current amplitudes by taking (α, G_μ, M_Z) as the set of independent parameters, where G_μ is the Fermi constant measured in muon decay.²⁶ In this case, the only explicit dependence on m_f^{internal} logarithms arise from $F_A^{(4)}$.

In summary, we conclude that $F_A^{(4)}$ generates the largest contribution to R in PNC scattering involving a charged-lepton vector current and that the relative importance of other radiative corrections depends on the specific process under consideration.

V. ANAPOLE MOMENTS OF $T_3^L=0$ HADRONS

At the simplest, “single particle” level of approximation, F_A/M^2 for a hadron is just a spin-flavor weighted

sum of the AM’s of the constituent quarks. Because the constituent quark AM’s are gauge-dependent, the AM of a hadron, which we denote F_A^{had} , is in general not well defined. It has unambiguous physical meaning only in the context of a physical amplitude, such as the amplitude for lepton-nucleon scattering, in which other ξ -dependent radiative corrections involving a single quark line cancel the ξ dependence of the quark AM (Fig. 6). We refer to the full set of one-loop corrections of Fig. 6 involving a single quark line and an external probe as “one-quark” radiative corrections. Similarly, we denote the individual quark AM contributions to F_A^{had} as the “one-quark” component, $F_A^{\text{one-quark}}$. Contributions from $F_A^{\text{one-quark}}$ to a complete scattering amplitude are illustrated in Figs. 6(a) and 6(b), with $V=\gamma$ and $V'=Z^0$.

Most of the conclusions discussed above with regard to the elementary fermion AM’s also carry over to $F_A^{\text{one-quark}}$. However, these conclusions must be modified in two respects for hadrons which have *weak* isospin quantum number $T_3^L=0$ (e.g., hadrons composed solely of equal numbers of u and d quarks). First, both of the gauge-dependent terms $F_A^{(1)}$ and $F_A^{(2)}$ are proportional to the axial-vector quark- Z^0 coupling, $g_A^q = -2T_3^{\text{quark}}$. Consequently, for any hadron whose $SU(2)_L$ quantum number $T_3^L=0$, the ξ -dependent components of the constituent quark AM’s sum to zero. The remaining ξ -independent one-quark contributions generate a well-defined AM of the $T_3^L=0$ hadron. In the valence-quark picture of hadrons, for example, one could speak of a well-defined AM of the ρ^0 vector meson or of a well-defined strong isoscalar component of the nucleon AM.

Second, because $F_A^{(4)}$ is also proportional to g_A^q , it does not contribute to an $F_A^{\text{had}}(T_3^L=0)$. The only nonvanishing one-quark contribution comes from $F_A^{(3)}$, which contains the external-mass logarithms. Formally speaking, this result implies that the contribution made by an $F_A^{\text{had}}(T_3^L=0)$ to physical amplitudes can be distinguished from all other contributions in the limit that $m_f^{\text{external}} \rightarrow 0$. All other contributions entering at similar or lower order in electroweak couplings are finite for vanishing m_f^{external} . Thus, in a world where m_f^{external} were infinitesimally small, the term proportional to F_A^{had}/M^2 of a $T_3^L=0$ hadron would dominate any scattering amplitude to which it contributes. In this formal limit, $F_A^{\text{had}}(T_3^L=0)$ would

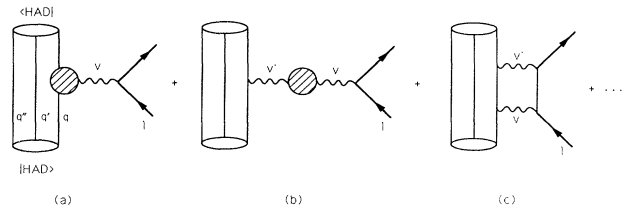


FIG. 6. One-quark contributions to second-order semileptonic scattering amplitudes. All electroweak interactions involve a single-quark line and the lepton probe (l). V and V' have the same meaning as in Fig. 2. For $V=\gamma$ and $V'=Z^0$, (a) and (b) represent the contribution made by $F_A^{\text{one-quark}}$ to the full amplitude.

satisfy our definition of a physical observable.

Even though it is a well-defined quantity, $F_A^{\text{had}}(T_3^L=0)$ is not necessarily distinguishable away from the $m_f^{\text{external}} \rightarrow 0$ limit. In the case of parity-violating, semi-leptonic scattering from isoscalar hadrons, for example, the $V(l^\pm) \times A(\text{had})$ amplitude receives contributions from both the $F_A^{(3)}$ of the quarks and the two boson-exchange diagrams. All other one-loop electroweak corrections, as well as the three-level Z^0 -exchange term, are proportional to g_A^q and, therefore, do not contribute. When constituent quark masses are used for the m_q^{external} , the isoscalar part of the two-boson-exchange contribution is roughly twice the isoscalar F_A^{had} term.²⁷ We conclude, then, that although $F_A^{\text{had}}(T_3^L=0)$ is ξ independent and would be observable in the unphysical $m_f^{\text{external}} \rightarrow 0$ limit, in the real world there is no way to isolate it from other electroweak radiative corrections.

We emphasize that these conclusions apply only to hadronic systems satisfying $T_3^L=0$. Naively, one might also expect the AM's of hadrons having *strong* isospin quantum number $T_3^{\text{strong}}=0$ to be well defined. The presence of sea quarks in hadrons, however, implies otherwise. To see why, consider the nucleon. Both theoretical predictions²⁸ as well as results from ν - p and deep-inelastic μ - p scattering experiments^{29,30} suggest that $\langle N | \bar{s} \gamma_\mu \gamma_5 s | N \rangle \neq 0$. Since one expects matrix elements of the c -, t -, and b -quark axial-vector current matrix elements to be significantly suppressed with respect to light-quark matrix elements,²⁸ these results imply that a $T_3^{\text{strong}}=0$ nucleon system such as the deuteron does not satisfy $T_3^L=0$. Consequently, the AM of such a system receives ξ -dependent contributions from sea s quarks, rendering the total AM undefined. Similar conclusions hold for other $T_3^{\text{strong}}=0$ hadrons as well. The AM's of such hadrons would be physical observables in the $m_f^{\text{external}} \rightarrow 0$ limit only if $\langle \text{had} | \bar{s} \gamma_\mu \gamma_5 s | \text{had} \rangle = 0$.

VI. NUCLEON ANAPOLE MOMENTS

Weak interactions among bound, hadronic quarks generate additional radiative corrections beyond those illustrated in Fig. 6. We denote this new set of corrections, illustrated in Fig. 7, as “many-quark” effects. These effects induce contributions to scattering amplitudes from a plethora of hadronic intermediate states not present in the simple one-quark picture of Fig. 6. Axial hadronic corrections to the γ -hadron coupling, as in Figs. 7(a) and 7(b), correspond to a many-quark component of the had-

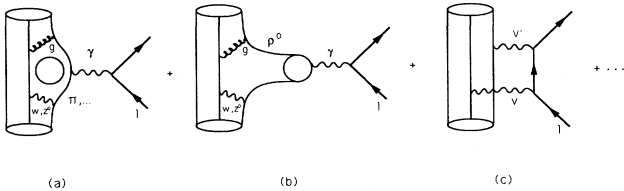


FIG. 7. Many-quark radiative corrections, generated by weak interactions among bound, hadronic quarks. Contributions as in (a) and (b) illustrate axial-vector corrections to the γ -hadron vertex which induce a many-quark term in the hadron AM.

ron AM, $F_A^{\text{many-quark}}$. In light of the role played by individual quark AM's in both F_A^{had} as well as in its contribution to physical scattering processes, it is interesting to consider $F_A^{\text{many-quark}}$ from the same perspective. In particular, one would like to know how large a contribution weak quark-quark interactions make to F_A^{had} , at what scale $F_A^{\text{many-quark}}$ enters physical amplitudes, whether $F_A^{\text{many-quark}}$ is gauge dependent, and whether it is distinguishable—either formally or numerically—from other radiative corrections.

Because a first-principles treatment of low-energy strong interactions among hadronic quarks is at present intractable, one must rely on effective theories of hadronic interactions in attempting to study the properties of $F_A^{\text{many-quark}}$. To that end, we focused on the nucleon AM, F_A^N , and calculated the contributions made by the diagrams in Figs. 8 and 9 as representative of the size of such effects. We refer to these contributions as the “meson cloud” component of the nucleon AM, $F_A^{\text{meson cloud}}$. The meson-nucleon intermediate states appearing in Figs. 8 and 9 are generated by strong and weak interactions among the nucleon constituents, interactions for which the meson-nucleon vertices constitute an effective, low-energy parametrization. The strong, pseudovector π - N coupling, $g_{\pi NN}/2m_N$, is determined from low-energy scattering to give³¹ $g_{\pi NN} \approx 13.45$ and the ρ - γ transition amplitude is estimated from vector dominance to be³² $C_{\rho\gamma} = e/g_{NN\rho}$ with $g_{NN\rho}^2 \approx (4\pi) \times 2.2$.

The weak meson-nucleon couplings h_{NNM} give the amplitude for PNC decay of a nucleon (N) into a nucleon and meson ($N' + M$). Their presence in Fig. 8 render the resulting photon-nucleon coupling axial vector in character. “Reasonable ranges” of values of the h_{NNM} have been derived using quark-model methods by Desplanques, Donoghue, and Holstein³³ (DDH), while the standard, theoretical analyses of nuclear parity-violation experiments have placed some constraints on the PNC couplings.³⁴ At present, the DDH estimates and the results of nuclear parity violation allow for considerable latitude in the values of the h_{NNM} . This lack of knowledge of the PNC couplings introduces considerable

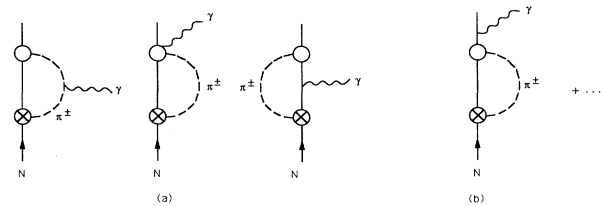


FIG. 8. Pion-loop contribution to the nucleon AM. The associated amplitude represents a low-energy, effective theory model of the hadronic part of the process illustrated in Fig. 7(a). Open circles denote parity-conserving couplings, and crossed circles represent PNC meson-nucleon couplings. Electromagnetic gauge invariance requires a photon insertion in all charged-particle lines. The $NN\pi\gamma$ vertex results from performing a minimal substitution in the strong, pseudovector $NN\pi$ coupling.

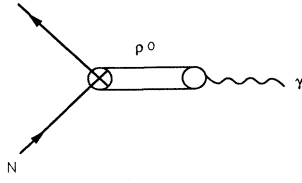


FIG. 9. ρ -meson-pole contribution to the nucleon AM. The crossed circle denotes the PNC N - ρ^0 coupling. The ρ^0 - γ transition amplitude (open circle) is estimated using the vector-dominance model for the parity-conserving nucleon form factor. This diagram models hadronic processes of the type illustrated in Fig. 7(b).

uncertainty into our estimates for $F_A^{\text{meson cloud}}$.

Because theoretical treatments of the h_{NNM} identify them with the amplitude for *decay* processes ($N \rightarrow N' + M$) involving on-shell particles, they do not depend on the choice of weak gauge. On-shell matrix elements represent physical amplitudes and cannot, therefore, depend on an unphysical gauge parameter. Consequently, our estimates of the amplitudes associated with Figs. 8 and 9 are ξ independent. In principle, the vertices

appearing in Fig. 8 contain additional, ξ -dependent terms not considered in our calculation since the intermediate hadronic states involve off-shell (unphysical) particles. Inclusion of such off-shell contributions to the h_{NNM} would require the presence of other diagrams in order to obtain an overall ξ -independent result for any physical amplitude in which these diagrams appear. Since we are interested primarily in determining the scale of many-quark effects rather than in performing a definitive numerical calculation, we did not include such off-shell effects.

Details of the π -loop and ρ^0 -pole calculations appear in the Appendix. Recalling that for nucleons $M = m_N$ in Eq. (1), we obtain, for the F_A from Figs. 8 and 9,

$$F_A^{\pi \text{ loop}} = - \left[\frac{f_\pi g_{\pi NN}}{8\sqrt{2}\pi^2} \right] (\alpha_S + \alpha_V \tau_3),$$

$$\alpha_S = F_1(0) + \frac{1}{2}[F_2(0) - F_3(0)], \quad (10)$$

$$\alpha_V = \frac{1}{2}[F_3(0) - F_2(0)],$$

where

$$F_1(0) = \frac{1}{3} \left[\frac{5}{2} - x_\pi^2 + (3 - 4x_\pi^2 + x_\pi^4) \ln x_\pi + \frac{(2 - x_\pi^2)(1 - 4x_\pi^2)}{x_\pi(4 - x_\pi^2)^{1/2}} \mathcal{F}(x_\pi) \right] \rightarrow \frac{2}{3} + \ln x_\pi + \frac{\pi}{6} \frac{1}{x_\pi} + \mathcal{O}(x_\pi^2),$$

$$F_2(0) = \frac{1}{3} \left[\frac{1}{2} + x_\pi^2 + x_\pi^2(1 - x_\pi^2) \ln x_\pi - \frac{x_\pi^3(3 - x_\pi^2)}{(4 - x_\pi^2)^{1/2}} \mathcal{F}(x_\pi) \right] \rightarrow \frac{1}{6} + \mathcal{O}(x_\pi^2), \quad (11)$$

$$F_3(0) = 1 - x_\pi^2 \ln x_\pi - \frac{x_\pi(2 - x_\pi^2)}{(4 - x_\pi^2)^{1/2}} \mathcal{F}(x_\pi) \rightarrow 1 + \mathcal{O}(x_\pi^2),$$

$$x_\pi \equiv \frac{m_\pi}{m_N},$$

$$\mathcal{F}(x_\pi) \equiv \arctan \left[\frac{x_\pi}{(4 - x_\pi^2)^{1/2}} \right] + \arctan \left[\frac{2 - x_\pi^2}{x_\pi(4 - x_\pi^2)^{1/2}} \right], \quad (12)$$

and

$$F_A^{\rho \text{ pole}} = - \left[\frac{m_N}{m_\rho} \right]^2 \frac{1}{g_{NN\rho}} (h_\rho^s + h_\rho^v \tau_3),$$

$$h_\rho^s \equiv h_\rho^{(1)}, \quad (13)$$

$$h_\rho^v \equiv h_\rho^{(0)} + \frac{1}{\sqrt{6}} h_\rho^{(2)}.$$

Here, f_π and $h_\rho^{(i)}$ denote the weak $NN\pi$ and $NN\rho$ couplings, respectively, with the values of $i=0, \dots, 2$ corresponding to different isospin channels in the $N \rightarrow N' + \rho$ decay amplitude (the weak $NN\pi$ coupling, conventionally denoted by f_π rather than $h_{NN\pi}$ in the literature, is not to be confused with the pion decay constant).

The result in Eqs. (10)–(12) was obtained independently

by Haxton and Henley, who used pseudoscalar rather than pseudovector coupling at the strong $NN\pi$ vertex.¹⁰ Use of pseudovector coupling renders the pion loop integrals corresponding to Fig. 8(a) linearly divergent. The QED Ward identities guarantee that the sum of these linearly divergent vertex corrections to the self-energy amplitudes in Fig. 8(b) is UV finite.²⁷ However, the UV finite part of linearly divergent integrals depends on one's choice for routing of loop momentum,¹⁶ and an auxiliary condition must be imposed in order to define the amplitude. In the present case, we require the sum of amplitudes 8(a) and 8(b) to have the current-conserving form of the anapole term in Eq. (1). We obtain this form by subtracting a term associated with the ambiguity loop-momentum routing. Our procedure is discussed in more detail in the Appendix.

From the results in Eqs. (10)–(13) we observe first the dependence of $F_A^{\text{meson cloud}}$ on parameters characteristic of hadronic physics: strong and weak hadronic couplings as well as hadronic masses. The chiral limit ($m_\pi \rightarrow 0$) of $F_A^{\pi \text{ loop}}$ given in Eq. (11) shows the leading m_π dependence of the nucleon AM. This dependence on hadronic masses and couplings illustrates how the scale of the many-quark component of F_A^{had} is determined by parameters which do not enter either the lepton AM's or the one-quark terms in F_A^{had} . In particular, we note that $\langle r^2 \rangle_5^{\text{em}} \sim M_V^{-2}$ for leptons and quarks, where $V = M_Z, M_W$, whereas the scale of $\langle r^2 \rangle_5^{\text{em}}$ for hadrons is set in part by M_{had}^{-2} (although a $M_{Z,W}^{-2}$ dependence is implicit in the h_{NNM} , which represents the effects of W and Z^0 exchange between hadronic quarks).

The formulas in (10)–(13) also suggest another formal limit in which the nucleon AM could be considered a physical observable. As m_π and $m_\rho \rightarrow 0$, $F_A^{\text{meson cloud}}$ diverges. For sufficiently small meson masses, then, $F_A^{\text{meson cloud}}$ will dominate interactions in which a charged particle probes an axial nucleon current. To $O(\alpha G_F)$, no other m_π and m_ρ singularities appear in the $V(l^\pm) \times A(N)$ amplitude. In this special (and unphysical) limit, the $T_3^L = 0$ component of the nucleon AM would be both well defined and distinguishable from other, second-order electroweak corrections. In principle, one could perform electron-scattering experiments on proton and neutron targets (or deuterium) to isolate this term. At the physical values of m_π and m_ρ , however, the total nucleon AM, $F_A^{\text{one-quark}} + F_A^{\text{meson cloud}}$, does not necessarily dominate amplitudes to which it contributes, so that F_A^N cannot be considered an observable away from the $m_{\text{meson}} \rightarrow 0$ limit. Contributions from $F_A^{\text{meson cloud}}$ to PNC $V(e) \times A(N)$ scattering amplitudes, for example, enter at the same scale as other one-quark radiative corrections.¹⁸

Although we have explicitly calculated the loop and pole diagrams only for the lightest pseudoscalar and vector meson, respectively, we expect similar contributions to result from loops and pole graphs involving the other lowest-lying mesons as well. Like the terms in Eqs. (10)–(13), contributions from these other mesons should diverge as $m_{\text{meson}} \rightarrow 0$, thereby rendering $F_A^N(T_3^L = 0)$ a physical observable in this limit. However, in the real world, we expect the pion-loop and ρ -pole diagrams to generate the leading meson-cloud contribution to the nucleon AM. The chiral limit in Eq. (11) suggests that contributions from loops involving heavier mesons will be suppressed by roughly m_π/m_{heavy} , where m_{heavy} is the mass of any meson heavier than the pion. Similarly, other vector-meson resonance terms should be down from (13) by roughly $(m_\rho/M'_{VM})^2$, where M'_{VM} is the mass of any neutral vector meson other than the ρ^0 . Contributions from intermediate states involving nucleon resonances or more than one meson should also be suppressed, since the masses associated with such states lie at considerably higher energies. These conclusions could be modified if the h_{NNM} and parity-conserving couplings for heavier mesons, as well as those corresponding to nucleon resonances and multimeson states, are

significantly larger than those for the π and ρ .

We conclude our discussion of F_A^N by emphasizing some of the ambiguities and uncertainties associated with our calculations. First, from the standpoint of principle, one should question the believability of any one-loop calculation involving hadrons. One-loop diagrams arise formally in the context of a *perturbative* expansion of the full amplitude, whereas the π -loop amplitude already involves one power of a large coupling ($g_{\pi NN}$). Moreover, the vertices appearing in Fig. 8 are appropriate to π - N interactions in the low-energy momentum regime, whereas the loop integral involves integration over all energy-momentum scales. Conceivably, higher-derivative terms in the strong and weak π - N interactions could play a significant role at high-momentum scales. These caveats imply that one should not place too much emphasis on the precise numerical result for $F_A^{\pi \text{ loop}}$.

Even with these qualifications in mind, however, one still has reason to derive some physical insight from the result in Eqs. (10)–(12). Pion-loop estimates of the nucleon anomalous magnetic moments, for example, generate at least the correct *scale* of the κ_N ,³⁵ suggesting that $F_A^{\pi \text{ loop}}$ may correctly set the *scale* of pionic contributions to F_A^N . Moreover, the $1/m_\pi$ and $\ln(m_\pi/m_N)$ infrared singularities in (10)–(12) imply that the loop integrals receive their dominant contributions from low-momentum regions where the effect of any higher-derivative terms in the $NN\pi$ couplings should be negligible. Finally, this estimate is instructive since it illustrates the characteristic dependence on physical parameters and couplings ($m_N, m_\pi, g_{\pi NN}, h_{NN\pi}$) of a particular physical effect (pion cloud).

The believability of the $F_A^{\rho \text{ pole}}$ is perhaps less questionable, given that no loop integration and no expansion in a large coupling are involved in the amplitude for Fig. 9. Moreover, the vector dominance model for the isovector nucleon form factor $F_1(q^2)$, in which the PNC $NN\rho$ vertex of Fig. 9 is replaced by the strong $NN\rho$ coupling, reproduces quite closely the experimentally determined q^2 dependence of F_1 .³² This success of the vector-dominance model provides some support for the believability of the estimate (13).

In addition to these questions of principle, the latitude in allowed values for the h_{NNM} introduce significant uncertainties into numerical estimates based on (10)–(13). In the case of $V(e) \times A(N)$ scattering, the resulting uncertainty in the contribution of $F_A^{\text{meson cloud}}$ to the radiative correction R is of the same order of magnitude as $R^{\text{meson cloud}}$ itself, when the latter is estimated using the DDH “best values” for the h_{NNM} .¹⁸

From these observations we conclude that the nucleon AM, though not an observable due to the ξ dependence of the valence-quark AM's, does contain ξ -independent components which are qualitatively distinct from the single quark component. These many-quark terms diverge as $m_{\text{meson}} \rightarrow 0$ and would dominate scattering amplitudes in this limit. To the extent one can neglect the presence of heavy quarks in the nucleon, the isoscalar nucleon AM is well-defined and satisfies the definition of a physical observable for vanishing m_{meson} . However, at the physical

values of m_{meson} , contributions from $F_A^{\text{many-quark}}$ enter at the same scale as other second-order electroweak effects and are not, therefore, experimentally distinguishable. The presence of these components in the nucleon AM introduces significant theoretical uncertainty into radiative corrections to $V(e) \times A(N)$ scattering.

VII. NUCLEAR ANAPOLE MOMENTS

We conclude with a brief discussion of one physically realizable case for which it can make sense to treat an AM as distinct from other second-order, electroweak effects: the AM's of nuclei. Since this case has been treated in more detail elsewhere,^{9,10} we limit our remarks to a comparison of the nuclear AM with the lepton, quark, and nucleon AM's. In doing so, we delineate between one-body ($F_A^{\text{one-body}}$) and many-body ($F_A^{\text{many-body}}$) components of F_A^{nuclear} , where $F_A^{\text{one-body}}$ denotes the component generated by a spin-isospin weighted sum of the single nucleon AM's and where $F_A^{\text{many-body}}$ results from weak interactions among the bound nucleons. This separation into one- and many-body components of F_A^{nuclear} is analogous to our earlier separation of F_A^{nuclear} into one-

and many-quark terms. Several features of F_A^{nuclear} merit comment.

First, the nuclear AM is both ξ dependent and renormalization-scheme dependent since it receives contributions from the ξ -dependent nucleon (quark) AM's. Consequently, F_A^{nuclear} is in general not well defined and has no physical meaning apart from scattering amplitudes. However, for idealized nuclei satisfying $T_3^L=0$ F_A^{nuclear} is well defined and would meet both criteria defining physical observables when any of the zero-mass limits ($m_f^{\text{external}} \rightarrow 0$ and $m_{\text{meson}} \rightarrow 0$) discussed above is taken. We note that these statements are consequences of the one-body component of F_A^{nuclear} alone.

Second, $F_A^{\text{one-body}}$ is independent of the nuclear radius (or mass number, A) and is dominated by the AM of an unpaired valence nucleon. These features follow from the form of the anapole term in Eq. (1), which reduces to $Q^2\sigma - Q\sigma \cdot Q$ ($Q=q$) in the nonrelativistic limit. The dependence on σ implies that only the AM of a nucleon with an unpaired spin will contribute to $F_A^{\text{one-body}}$. The factors of Q become derivatives in the one-body, coordinate-space current operator generated by the nucleon AM:

$$\mathbf{J}(x_1, \dots, x_A; r)_{\text{anapole}}^{\text{one-body}} = -\frac{e}{m_N^2} \sum_{i=1}^A [F_A^N(0)^S + F_A^N(0)^V \tau_3(i)] [\sigma(i) \nabla_r^2 - \sigma(i) \cdot \nabla_r \nabla_r] \delta(\mathbf{r} - \mathbf{x}_i). \quad (14)$$

Here, r is the coordinate at which the virtual photon probes the nucleus, x_i is the position of the i th nucleon, and $F_A^N(0)^{S(V)}$ is the isoscalar (isovector) nucleon anapole moment. After inserting the current (14) into the multipole projection of Eq. (3), one may integrate the ∇_r operators twice by parts onto the r^2 , reducing it to a constant. Consequently, the scale of $F_A^{\text{one-body}}/M^2$ is set predominantly by the parameters governing the size of the single-nucleon AM rather than by the spatial extent of the nucleus.

These one-body properties of F_A^{nuclear} are significantly modified by the many-body physics of the nucleus. In particular, weak, PNC N - N interactions, mediated by the exchange of the lightest, nonstrange pseudoscalar and vector mesons (Fig. 10), generate a gauge-independent component of $F_A^{\text{many-body}}$ whose magnitude grows as the square of the nuclear radius: $F_A^{\text{many-body}} \sim \langle R^2 \rangle \sim A^{2/3}$. This $A^{2/3}$ effect results from both parity mixing in nuclear states⁹ and from PNC meson-exchange currents.¹⁰ In the $A \rightarrow \infty$ limit, then $F_A^{\text{many-body}}$ will be formally distinguishable from other second-order electroweak effects, since it will dominate neutral-current-scattering amplitudes in this case. To leading nontrivial order in G_F , all other contributions to $V(I^\pm) \times A(\text{nucleus})$ are essentially independent of A . Taking $A \rightarrow \infty$ in $T_3^L=0$ nuclei constitutes the third unphysical limit in which an AM could be considered a well defined and physically distinguishable quantity.

In contrast with the formal limits considered previously, however, the $A \rightarrow \infty$ limit is approximated rather well by certain nuclear systems in the real world. Indeed, for

finite values of A , $F_A^{\text{many-body}}$ can generate the leading term in physical amplitudes, depending on the nucleus under consideration. The dominance of $F_A^{\text{many-body}}$ can occur in two ways: (a) the nucleus is sufficiently heavy, or (b) near degeneracies in opposite-parity nuclear states enhances the parity-mixing contribution. Examples of each case were reported in Ref. 10. The π -exchange term in the $F_A^{\text{many-body}}$ of ^{133}Cs generates a contribution to $V(e) \times A(\text{nucleus})$ scattering roughly three times as large as the tree-level, Z^0 -exchange term. In fact, recent atom-

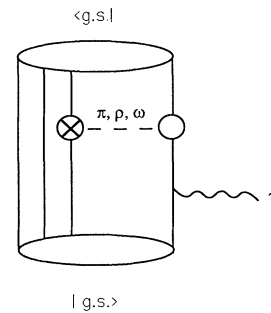


FIG. 10. Weak, PNC N - N interactions responsible for the many-body component of the nuclear AM. Meson-nucleon couplings have the same meaning as in Figs. 8 and 9. Solid lines represent constituent nucleons of a nucleus with ground state $|g.s.\rangle$. Different time orderings for the nuclear Green's function generate parity-mixing and exchange-current contributions to $F_A^{\text{many-body}}$.

ic parity-violation measurements on ^{133}Cs provide the first experimental evidence for a large $F_A^{\text{many-body}}$ having a magnitude consistent with theoretical predictions.² In the case of ^{19}F , mixing of a 110-keV opposite-parity state into the ground state enhances $F_A^{\text{many-body}}$ over its $A^{2/3}$ scale by roughly a factor of 2. The resulting contribution to $V(e) \times A(\text{nucleus})$ scattering amplitude is of the same order of magnitude as the tree-level term. In both of these cases, $F_A^{\text{many-body}}$ will be the dominant $O(\alpha G_F)$ effect in any nuclear-spin-dependent, neutral-current process. Although for neither of these nuclei is the total AM well defined (since neither is an isoscalar system), the distinct physical origin of $F_A^{\text{many-body}}$, as well as its surprisingly large contribution to PNC scattering amplitudes, provides some justification for distinguishing it from other second-order, electroweak effects.

VIII. CONCLUSIONS

We have shown that in the context of the minimal standard model, the NCR and AM of fermionic systems are not, in general, well defined and cannot be considered physical observables. Low- to intermediate-energy measurements sensitive to second-order, electroweak amplitudes cannot isolate an AM (NCR) from other $O(\alpha G_F)$ effects. However, for fermionic systems satisfying $T_3^L=0$ —such as a deuteron in which the presence of heavy quarks in the sea is neglected—the AM is well defined. We have argued, moreover, that the AM of various $T_3^L=0$ systems could be observed experimentally in a world defined by one of the following mathematical limits: (i) $m_f^{\text{external}} \rightarrow 0$, for a general fermionic system; (ii) $m_{\text{meson}} \rightarrow 0$, for nucleons; (iii) $A \rightarrow \infty$, for nuclei. In each of these special cases, the AM would dominate any scattering amplitude to which it contributes and could, on the basis of our definition, be considered an “observable.” In the actual world, only the third limit is approximated by nature. The many body AM’s of heavy and/or nearly degenerate nuclei may, in fact, generate the leading term in PNC amplitudes. From this standpoint, one might think of $F_A^{\text{many-body}}$ as a quasiobservable. Indeed, measurements of the gauge-independent $F_A^{\text{many-body}}$ —even in $T_3^L \neq 0$ nuclei for which the *total* AM is not well defined—could provide new insight into the weak, N - N interaction.

ACKNOWLEDGMENTS

We thank Professor S. B. Treiman, Professor J. F. Donoghue, Professor W. C. Haxton, Professor E. M. Henley, and Professor X. Ji for helpful discussions. This research was supported in part by grants from the National Science Foundation and the U.S. Department of Energy.

APPENDIX: MESON-CLOUD CONTRIBUTIONS

In this appendix, we discuss technical aspects of the π -loop and ρ^0 -pole calculations. Specifically, we give the effective nucleon-meson couplings used in estimating the amplitudes associated with Figs. 8 and 9 and show (i)

how the ambiguity associated with the linear divergence in the π -loop graph may be handled in such a way as to obtain the current-conserving form of the anapole term in Eq. (1), and (ii) how the QED Ward identities guarantee that the sum of vertex graphs in Fig. 8(a) with the self-energy diagrams of 8(b) is UV finite and gauge invariant, once the linear divergence is properly handled.

Pion loop

The low energy, effective $NN\pi$ strong and weak interaction used in the π -loop calculation are given by

$$\begin{aligned} \mathcal{L}_{NN\pi}^{\text{strong}} &= -\frac{g_{\pi NN}}{2m_N} \bar{N} \gamma_\mu \gamma_5 \tau \cdot (\partial^\mu \pi) N, \\ \mathcal{L}_{NN\pi}^{\text{weak PNC}} &= -\frac{f_\pi}{\sqrt{2}} \bar{N} (\tau \times \pi)_3 N, \end{aligned} \quad (15)$$

where

$$N \equiv \begin{pmatrix} p \\ n \end{pmatrix}$$

and π are the nucleon and pion fields, respectively. Electromagnetic couplings are obtained by performing the minimal substitution $\partial_\mu \rightarrow \partial_\mu - ieQ A_\mu$ in the usual nucleon and meson kinetic energy Lagrangians as well as in the pseudovector (PV) $NN\pi$ interaction in (15). In the latter case, this substitution generates the $NN\pi\gamma$ “seagull” vertex appearing in the second graph of Fig. 8(a).

When PV coupling is used for the strong $NN\pi$ vertices in Fig. 8, a simple power counting argument implies that the vertex-correction loop integrals are linearly divergent. It is well known that value of a linearly divergent loop integral is not, in general, well defined.³⁶ Different choices for the routing of loop momentum lead to different values for the amplitude. In particular, if we compute the integral once with momentum k assigned to one of the internal lines and compute it again with momentum $k+a$ ($a=\text{const}$) assigned to the same line, the two amplitudes will not necessarily agree:

$$\Lambda_{\mu 5}(k+a) - \Lambda_{\mu 5}(k) \equiv \Delta_{\mu 5}(a) \neq 0,$$

where $\Lambda_{\mu 5}(k) \equiv \int d^4k I_{\mu 5}(k)$ denotes the loop integral with integrand $I_{\mu 5}(k)$.³⁷ In order to obtain a well-defined amplitude, one must impose some auxiliary condition. In the case of the amplitude associated with Fig. 8, we require conservation of $\langle p' | J_\mu^{\text{em}}(0) | p \rangle$. Imposing this condition, in effect, defines the routing of loop momentum.

For a linearly divergent integral in four space-time dimensions, the ambiguity $\Delta_{\mu 5}(a)$ is given by¹⁶

$$\Delta_{\mu 5}(a) = 2i\pi^2 a^\lambda \lim_{R \rightarrow \infty} R^2 R_\lambda I_{\mu 5}(R), \quad (16)$$

where R is the radius of a four-dimensional hypersphere defining the volume over which the loop momentum is integrated. Applying (16) to the integrals associated with the first two vertex graphs of Fig. 8(a), we find that they give $\Delta_{\mu 5}(a)=0$. For the third graph, in which the photon is inserted into the intermediate nucleon line, the loop integral is

$$\Lambda_{\mu 5} \propto -i \int \frac{d^4 k}{(2\pi)^4} \frac{1}{(p'+k)^2 + m_N^2} \frac{1}{(p+k)^2 + m_N^2} \frac{1}{k^2 + m_\pi^2} \\ \times \{ (2m_N^2 + k^2) [\gamma_\mu, \not{k}] + 2m_N k^2 \gamma_\mu + 4m_N \not{k} k_\mu \\ - 2m_N (\gamma_\mu \not{p} \not{k} + \not{k} \not{p}' \gamma_\mu) \\ + \not{k} (\gamma_\mu \not{p} - \not{p}' \gamma_\mu) \not{k} \} \gamma_5, \quad (17)$$

where a Wick rotation to Euclidean space has been performed. We employ a cutoff Λ as a regulator instead of the more common dimensional regularization to avoid any ambiguities associated with the continuation of γ_5 to $4-\epsilon$ dimensions. Application of (16) to the integrand of (17) gives

$$\Delta_{\mu 5}(a) \propto i [\not{a}, \gamma_\mu] \gamma_5$$

sandwiched between two on-shell nucleon spinors. Since there are two independent momenta associated with the vertex graphs, say $q \equiv p - p'$ and $P \equiv p + p'$, we may write $a = \alpha P + \beta q$. Different choices of α and β correspond to different routings of the loop momentum. In this case we have

$$\Delta_{\mu 5} \propto i\alpha [\not{P}, \gamma_\mu] \gamma_5 + i\beta [\not{q}, \gamma_\mu] \gamma_5 \\ = i\alpha [\not{P}, \gamma_\mu] \gamma_5 - 2\beta \sigma_{\mu\nu} q^\nu \gamma_5$$

where we have used $[\not{q}, \gamma_\mu] = 2i\sigma_{\mu\nu} q^\nu$. The second term, which is gauge invariant, is odd under CP transformations when sandwiched between two on-shell neutron or proton spinors. Since we have introduced no CP -violating terms into our effective strong, weak, and electromagnetic interactions, such a CP -odd term cannot arise from the loop integral. Thus, we must set $\beta \equiv 0$. The remaining term, which is not gauge invariant, gives the form of the ambiguity associated with the linear divergence in the vertex graphs.

Given this result, we may now write the general form of the vertex graphs of Fig. 8(a):

$$\text{Amp}|_{8(a)} = ie\bar{u}(p') \Lambda_{\mu 5} u(p)$$

with

$$\Lambda_{\mu 5} = A \gamma_\mu \gamma_5 + \frac{B(\alpha, q^2)}{m_N} [\not{P}, \gamma_\mu] \gamma_5 \\ + \frac{F_A(q^2)}{m_N^2} (q^2 \gamma_\mu - \not{q} q_\mu) \gamma_5. \quad (18)$$

In principle, the coefficients of the $q^2 \gamma_\mu \gamma_5$ and $-\not{q} q_\mu \gamma_5$ terms may differ, as they did for the vertex graphs in the elementary-fermion AM's. In the latter case, a longitudinal term in the Z - γ mixing tensor eliminated an extra gauge-noninvariant $\not{q} q_\mu \gamma_5$ term in the vertex graphs, resulting in a gauge-invariant form for the overall amplitude. In the present case, the self-energy diagrams of Fig. 8(b) are q_μ independent (so long as we do not use q^2 -dependent form factors at the em vertices), and no other graphs exist which are bilinear in q_μ . Hence, the terms bilinear in photon momentum must occur in the current-conserving form of the third term in Eq. (18).

In order to satisfy the requirement that

$q^\mu (\Lambda_{\mu 5}^{8(a)} + \Lambda_{\mu 5}^{8(b)}) = 0$, we must choose the momentum routing such that $B(\alpha, q^2) = 0$. In practice, we perform the momentum integration using a calculational convenient routing and subsequently identify and omit all terms proportional to $[\not{P}, \gamma_\mu] \gamma_5$. Since A and F_A are not affected by the choice of routing, identifying and omitting all terms of the form $[\not{P}, \gamma_\mu] \gamma_5$ is equivalent to choosing *a priori* a momentum routing consistent with the requirements of current conservation.

Having imposed electromagnetic gauge invariance to eliminate the linear divergence ambiguity, we now show how the QED Ward identities³⁸—which express gauge invariance—guarantee that the sum of the remaining terms in the vertex correction with the self-energy amplitudes of Fig. 8(b) generates a finite, gauge-invariant result. First, we observe that because the vertex graphs are *linearly* divergent, Weinberg's theorem on the asymptotic behavior of Green's functions³⁹ imply that the terms which diverge as the regulating cutoff $\Lambda \rightarrow \infty$ must be a polynomial of degree ≤ 1 in the external momenta. Since the second term in (18) has been eliminated by the choice of momentum routing and the third term is quadratic in photon momentum, all cutoff dependence must be contained in the first term.

Second, we note that the axial self-energy parts of diagrams 8(b) have the form

$$\text{Amp}|_{\text{self-energy}}^{\text{axial}} \equiv -i\Sigma^5(p) \equiv -i\Pi^5(p^2) \not{p} \gamma_5. \quad (19)$$

CP invariance forbids the presence of any $m_N \gamma_5$ term. From the QED Ward identity, we have

$$\Lambda_{\mu 5}(p, p) = -\frac{\partial \Sigma^5(p)}{\partial p^\mu} \\ = -\left[\Pi^5(p^2) \gamma_\mu + \frac{\partial \Pi^5(p^2)}{\partial p^\mu} \not{p} \right] \gamma_5. \quad (20)$$

Sandwiching this result between on-shell nucleon spinors and using the fact that $\bar{u}(p) \not{p} \gamma_5 u(p) = m_N \bar{u}(p) \gamma_5 u(p) = 0$, we have

$$\bar{u}(p) \frac{\partial \Sigma^5(p)}{\partial p^\mu} u(p) = \Pi^5(m^2) \bar{u}(p) \gamma_\mu \gamma_5 u(p) \quad (21)$$

for $p^2 = m_N^2$. Similarly, placing (18) [with $B(\alpha, q^2) = 0$] between on-shell spinors and using (20) and (21) gives

$$A = -\Pi^5(m_N^2). \quad (22)$$

Then, evaluating the self-energy diagrams of Fig. 8(b) with the photon inserted on either side of the loop gives, after some algebra,

$$\text{Amp}|_{8(b)} = ie\Pi^5(m_N^2) \bar{u}(p') \gamma_\mu \gamma_5 u(p) \\ = -ieA \bar{u}(p') \gamma_\mu \gamma_5 u(p) \quad (23)$$

using (22). Thus, the sum of 8(a) and 8(b) eliminates the remaining cutoff-dependent, gauge-noninvariant term in the total amplitude. Only the anapole term $\propto F_A/m_N^2$ survives.

Finally, we note that the terms in $F_A^N(q^2)^{\pi\text{-loop}}$ which diverge in the chiral limit ($m_\pi \rightarrow 0$) arise only from the

first diagram in Fig. 8(a). It is straightforward to show that these terms contribute only to the isoscalar component of F_A^N . From the forms (15) used for the effective N - π interactions, we have that the coupling for the PNC $n \rightarrow p \pi^-$ vertex has the opposite sign from the PNC $p \rightarrow n \pi^+$ vertex. The strong $n \rightarrow p \pi^-$ and $p \rightarrow n \pi^+$ vertices, on the other hand, have the same sign. Finally, the $\pi\pi\gamma$ vertex appearing in the first graph of Fig. 8(a) changes sign depending on whether the intermediate pion is a π^- or π^+ . Thus, this graphic has the same sign and magnitude whether the external nucleon is a proton or neutron (assuming $m_p = m_n$), so that its contribution to F_A^N is isoscalar.

ρ^0 -meson pole

We derive the vertices appearing in our ρ^0 -pole amplitude (Fig. 9) from the following PNC $NN\rho$ and PC ρ - γ interactions taken from Refs. 33 and 32, respectively:

$$\begin{aligned} \mathcal{L}_{NN\rho}^{\text{PNC}} &= \bar{N} \left[h_\rho^{(0)} \boldsymbol{\tau} \cdot \boldsymbol{\rho}_\mu + h_\rho^{(1)} \rho_\mu^3 \right. \\ &\quad \left. + \frac{h_\rho^{(2)}}{2\sqrt{6}} (3\tau_3 \rho_\mu^3 - \boldsymbol{\tau} \cdot \boldsymbol{\rho}_\mu) \right] \gamma^\mu \gamma_5 N, \\ \mathcal{L}_{\rho\gamma} &= \frac{1}{2} C_{\rho\gamma} F^{\mu\nu} \rho_{\mu\nu}^0, \end{aligned} \quad (24)$$

where ρ_μ is the ρ -meson field, $F_{\mu\nu}$ is the em field-strength tensor, and $\rho_{\mu\nu}^0 = \partial_\mu \rho_\nu^3 - \partial_\nu \rho_\mu^3$ and where $C_{\rho\gamma} = e/g_{NN\rho}$, $g_{NN\rho}$ being the strong $NN\rho$ coupling, is taken from the vector-dominance model for the em form factors of the nucleon and pion. We note that for the $NN\rho^0$ vertex, the PNC interaction in (24) may be written more simply as

$$\mathcal{L}_{NN\rho^0}^{\text{PNC}} = \bar{N} (h_\rho^s + h_\rho^v \tau_3) \rho_\mu^0 \gamma^\mu \gamma_5 N, \quad (25)$$

where

$$h_\rho^s = h_\rho^{(1)}, \quad (26)$$

$$h_\rho^v = h_\rho^{(0)} + \frac{1}{\sqrt{6}} h_\rho^{(2)}.$$

The DDH best values for the $h_\rho^{(i)}$ ($i=0, \dots, 2$) give $h_\rho^v/h_\rho^s \approx 80$ so that the ρ^0 -pole graph contributes mostly to the isovector nucleon AM, in contrast with the π loop, whose dominant contribution is isoscalar. We note also that $\mathcal{L}_{\rho\gamma}$ is manifestly gauge invariant, guaranteeing that the ρ^0 -pole amplitude has the current-conserving form of the anapole term in Eq. (1). The result for $F_A(0)^{\rho \text{ pole}}$ given in Eq. (13) is obtained by setting $q^2=0$ in the ρ^0 propagator.

-
- ¹Ya. B. Zeldovich, Zh. Eksp. Teor. Fiz. **33**, 1531 (1957) [Sov. Phys. JETP **6**, 1184 (1958)]; **39**, 115 (1960) [**12**, 177 (1961)].
- ²M. C. Noecker *et al.*, Phys. Rev. Lett. **61**, 310 (1988).
- ³R. Carlini and R. Siegel, in *Proceedings of the CEBAF 1987 Summer Workshop*, Newport News, Virginia, 1987, edited by F. Gross and C. Williamson (CEBAF, Newport News, 1987), p. 718.
- ⁴I. B. Khriplovich, University of Minnesota Report No. TPI-MINN-89/29-T, 1989 (unpublished).
- ⁵W. A. Bardeen, R. Gastmans, and B. Lautrup, Nucl. Phys. **B46**, 319 (1972).
- ⁶N. M. Monyonko and J. H. Reid, Prog. Theor. Phys. **73**, 734 (1985).
- ⁷J. L. Lucio, A. Rasado, and A. Zepeda, Phys. Rev. D **39**, 1091 (1985).
- ⁸G. Degrossi, A. Sirlin, and W. J. Marciano, Phys. Rev. D **39**, 287 (1989).
- ⁹V. V. Flambau, I. B. Khriplovich, and O. P. Sushkov, Phys. Lett. **146**, 367 (1984).
- ¹⁰W. C. Haxton, E. M. Henley, and M. J. Musolf, Phys. Rev. Lett. **63**, 949 (1989).
- ¹¹In treatments of electromagnetic transitions, this multipole is often referred to as the $E1$ multipole.
- ¹²A. J. F. Siegert, Phys. Rev. **52**, 787 (1937).
- ¹³J. L. Friar and S. Fallieros, Phys. Rev. C **29**, 1654 (1984).
- ¹⁴J. L. Friar and W. C. Haxton, Phys. Rev. C **31**, 2027 (1985).
- ¹⁵B. Kayser, Phys. Rev. D **26**, 1662 (1982).
- ¹⁶See, e.g., T. P. Cheng and L. F. Li, *Gauge Theory of Elementary Particle Physics* (Oxford University Press, New York, 1984), Chap. 9.
- ¹⁷K. I. Aoki, Z. Hioki, R. Kawabe, M. Konuma, and T. Muta, Suppl. Prog. Theor. Phys. **73**, 1 (1982).
- ¹⁸M. J. Musolf and B. R. Holstein, Phys. Lett. B **242**, 461 (1990).
- ¹⁹M. J. Musolf and B. R. Holstein (unpublished).
- ²⁰This definition of $\sin^2\theta_W$ is not unique. Alternate definitions may be used depending on the renormalization scheme in use. At one-loop order, different definitions of $\sin^2\theta_W$ need not be identical. For further discussion, see, e.g., Michael Peskin, in *Physics at the 100 GeV Mass Scale*, proceedings of the Seventeenth SLAC Summer Institute, Stanford, California, 1989, edited by E. C. Brennan (SLAC Report No. 361, Stanford, 1990).
- ²¹H. Czyz, K. Kolodziej, and M. Zralek, Can. J. Phys. **66**, 132 (1988).
- ²²Norman Dombey and A. D. Kennedy, Phys. Lett. **91B**, 428 (1980).
- ²³W. F. L. Hollik, Fortschr. Phys. **38**, 165 (1990).
- ²⁴W. J. Marciano and A. Sirlin, Phys. Rev. D **29**, 75 (1984).
- ²⁵We are indebted to Dr. X. D. Ji for clarification of this point.
- ²⁶A. Sirlin, Phys. Rev. D **22**, 971 (1980); W. J. Marciano and A. Sirlin, *ibid.* **22**, 2695 (1980).
- ²⁷M. J. Musolf, Ph.D. thesis, Princeton University, 1989.
- ²⁸J. Collins, F. Wilczek, and A. Zee, Phys. Rev. D **18**, 242 (1978).
- ²⁹L. A. Ahrens *et al.*, Phys. Rev. D **35**, 785 (1987).
- ³⁰European Muon Collaboration, J. Ashman *et al.*, Nucl. Phys. **B328**, 1 (1989).
- ³¹E. G. Adelberger and W. C. Haxton, Annu. Rev. Nucl. Part. Sci. **35**, 501 (1985).
- ³²J. J. Sakurai, *Currents and Mesons* (University of Chicago Press, Chicago, 1969).
- ³³B. Desplanques, J. F. Donoghue, and B. R. Holstein, Ann.

- Phys. (N.Y.) **124**, 449 (1980).
- ³⁴B. R. Holstein, *Weak Interactions in Nuclei* (Princeton Univ. Press, Princeton, NJ, 1989), Chap. 5; see also Adelberger and Haxton (Ref. 3).
- ³⁵H. A. Bethe and F. deHoffman, *Mesons and Fields* (Row, Peterson, and Co., Evanston, IL, 1955), Vol. II, p. 289ff.
- ³⁶R. Jackiw, in *Current Algebra and Anomalies* (Princeton Univ. Press, Princeton, NJ, 1985).
- ³⁷The subscript 5 indicates that the amplitude of interest (Fig. 8) is axial vector in character.
- ³⁸J. C. Ward, *Phys. Rev.* **78**, 1824 (1950); Y. Takashi, *Nuovo Cimento* **6**, 370 (1957).
- ³⁹S. Weinberg, *Phys. Rev.* **118**, 838 (1960).